

# Singularity-Free Constrained Steering Law for Triplet Control Moment Gyros

Rodrigo A. Zeledon<sup>1</sup> and Mason A. Peck<sup>2</sup>  
*Cornell University, Ithaca, NY, 14850*

Small CMGs are a power-efficient choice for the attitude actuation of small satellites. As in any other CMG implementation, dealing with kinematic singularities and other subtleties of implementation represents a challenge that must be overcome for such systems to realize their full potential. This paper describes the derivation and implementation of an online, singularity-free steering law for triplet arrays of CMGs—a configuration which has only recently received attention in the literature. The steering law is to be tested on Cornell University’s Violet satellite.

## Nomenclature

$C$	=	Constraint vector
$D$	=	Constraint term
$\hat{g}$	=	Gimbal axis unit vector
$h_1, h_2, h_3$	=	Momentum vector for CMG 1, 2 and 3
$h_x, h_y, h_z$	=	Array momentum in the x,y and z directions
$h_0$	=	Magnitude of momentum of each CMG
$I$	=	Moment of inertia of CMG rotor
$J$	=	Jacobian, $\partial\tau/\partial\Phi$
$K$	=	Gain matrix
$\tau$	=	Commanded torque vector
$\tau_x, \tau_y, \tau_z$	=	Commanded torque in the x, y and z directions
$\varphi_1, \varphi_2, \varphi_3$	=	Gimbal angle for CMG 1, 2 and 3
$\varphi_{1t}, \varphi_{2t}, \varphi_{3t}$	=	Gimbal angle for CMG 1, 2 and 3 in a trapezoidal configuration
$\Phi$	=	Vector of gimbal angles (made up of $\varphi_i$ )
$\omega$	=	CMG rotor angular velocity

## I. Introduction

CONTROL moment gyroscopes (CMGs) are momentum-exchange devices that can be used for attitude control of satellites. CMGs are particularly well suited for small satellites due to their low power consumption and high torque capacity.<sup>1</sup> Large CMGs have been used successfully in the International Space Station, but much smaller CMGs have also been proposed for the actuation of free-floating robots, for precise pointing of space-based telescopes, and for attitude control of small agile satellites<sup>2-6</sup>. NASA’s Manned Maneuvering Unit (MMU), for example, used small CMGs arranged in scissored pairs.<sup>3</sup>

A CMG is composed of a rotor and a motorized gimbal mounted perpendicular to the rotor’s spin axis. This arrangement allows the movement of the rotor’s momentum vector to be controlled through gimbal rate commands. For a single-gimbal configuration, each CMG’s momentum vector is constrained to a plane perpendicular to the gimbal axis and therefore several CMGs must be used to control all three axes.<sup>7</sup> In practice, at least four CMGs are used for three-axis control in order to avoid issues with singularities as well as for redundancy in case of failure. Kinematic singularities occur when the CMGs in an array are aligned such that there is at least one direction in

---

<sup>1</sup> Graduate Student, Department of Mechanical and Aerospace Engineering, 212 Kimball Hall, Ithaca, NY 14850, AIAA Student Member.

<sup>2</sup> Assistant Professor, Department of Mechanical and Aerospace Engineering, 212 Upson Hall, Ithaca, NY 14850, AIAA Full Member.

which torque cannot be generated. A singular configuration leads to loss of attitude control in at least one axis. Singularities are highly undesirable in a spacecraft design precisely because of this loss of control.

A CMG array produces the torque required for attitude control via an algorithm known as a steering law. This logic maps the torque commanded by the control law to the gimbal rates that the CMG must produce. For a steering law to be successful, it must meet the requirements presented in Ref. 8, summarized here. An ideal steering law should:

- 1) Introduce no torque error.
- 2) Be instantaneous, i.e. require no memory of the past or estimate of the future.
- 3) Respect the physical limits of the CMG.
- 4) Have no singularities.

In practice, the first requirement above means that the steering law should not avoid singularities by introducing errors in the torque generated. While considerable emphasis has been placed on developing methods to reduce the torque error near a singularity, such methods offer no guarantee that the array only remains in a singular configuration for a short period of time. If the array remains near a singular configuration for extended periods of time, torque errors can accumulate, resulting in poor attitude control. The second requirement rules out *a priori* knowledge of the torque commands, since for spacecraft attitude control these commands are likely part of a feedback loop and are not known perfectly beforehand. Thus, it is preferable to have a steering law that does not need to perform off-line calculations based on torque commands. The third requirement demands that the steering law never exceed some maximum gimbal rate. Finally, the steering law must also be able to avoid singular configurations, as discussed above. A survey of different types of steering laws for CMG control is presented in Ref. 7. Of these, the only ones which can meet the requirements above are null-motion approaches and constraint-based steering laws<sup>8</sup>.

This paper describes a constraint-based steering law for an array of six CMGs arranged as two orthogonal sets of “triplets” (as described in Ref. 8). An array so configured is also referred to in the literature as a “roof” array. Research performed at Honeywell<sup>10</sup> favors the roof configuration due to its inherent lack of elliptic singularities. Because a direct path exists from every point in the available momentum space to any other, the need for advanced trajectory planning is eliminated. Section II describes the triplet arrangement and the steering law for the array. Section III describes the validation techniques for this steering law, and the final section draws conclusions about the prospect for this steering logic.

## II. Triplet Arrays

### A. Description

A triplet array has three CMGs with parallel gimbal axes. The momentum vectors for these three CMGs lie in the same plane, which greatly simplifies the analysis of the CMGs. In order to span three dimensions, two triplet arrays must be used, with the gimbal axes of one triplet not parallel to the gimbal axes of the second triplet. In this paper the two triplets have orthogonal gimbal axes.

Each CMG has a rotor that spins at a rate  $\omega$ , which is constant in a reference frame fixed in the gimbal hardware. The momentum vector,  $h$ , is perpendicular to the face of the rotor and has scalar magnitude  $I\omega$ , where  $I$  is the moment of inertia of the rotor about its spin axis. The CMG can be gimballed, as shown in Fig. 1, about an axis  $\hat{g}$  perpendicular to the momentum vector. The rate at which the CMG is gimballed is denoted by  $\dot{\phi}$ .

Considering at first only one triplet, we

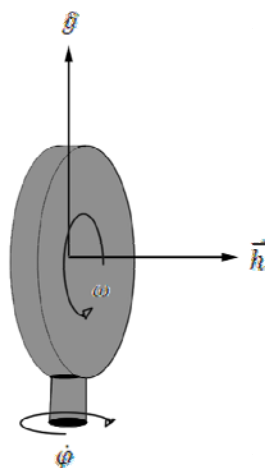


**Figure 1. Definition of vectors for single CMG.** The momentum vector,  $h$ , is the product of the rotor's inertia and the rotor speed,  $\omega$ .  $h$  is always perpendicular to the gimbal axis,  $\hat{g}$ . The gimbal rate is  $\dot{\phi}$ .

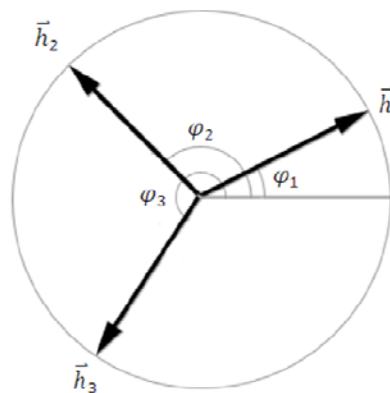


**Figure 2. Gimbal angles and momentum vectors for three CMGs in a triplet array.** The gimbal axis  $\hat{g}$  shown in Fig. 1 is out of the page. The three momentum vectors,  $h_1$ ,  $h_2$  and  $h_3$ , are constrained to the same plane in momentum space.

can define the gimbal rotation angles ( $\varphi_1$ ,  $\varphi_2$  and  $\varphi_3$ ) with respect to some arbitrary axis, as shown in Fig. 2. The total momentum vector would then be the vector sum of  $h_1$ ,  $h_2$  and  $h_3$ . This can be expressed in terms of the components of the total momentum vector as:

$$\begin{bmatrix} h_x \\ h_y \end{bmatrix} = h_0 \begin{bmatrix} \cos(\varphi_1) + \cos(\varphi_2) + \cos(\varphi_3) \\ \sin(\varphi_1) + \sin(\varphi_2) + \sin(\varphi_3) \end{bmatrix} \quad (1)$$

where  $h_0$  is the magnitude of the momentum for a single CMG, and assumed to be equal and constant for all CMGs. Note that the torque produced by the CMG array is the rate of change of the total momentum vector. A mapping from CMG gimbal rates to resulting torque can then be described by the Jacobian as<sup>8</sup>:

$$\begin{bmatrix} \tau_x \\ \tau_y \end{bmatrix} = h_0 \begin{bmatrix} -\sin(\varphi_1) & -\sin(\varphi_2) & -\sin(\varphi_3) \\ \cos(\varphi_1) & \cos(\varphi_2) & \cos(\varphi_3) \end{bmatrix} \begin{bmatrix} \dot{\varphi}_1 \\ \dot{\varphi}_2 \\ \dot{\varphi}_3 \end{bmatrix} = J(\Phi)\dot{\Phi} \quad (2)$$

Singularities occur when the Jacobian is not full-rank. That is, when  $\det(JJ^T)=0$ . For a triplet array, this occurs in two cases: when all three gimbal angles are equal, or when two gimbal angles are equal and the third is  $180^\circ$  from the other two<sup>10</sup>. The first case is known as a saturation singularity and occurs because the array has reached the momentum limit, where no more torque can be provided in the direction in which the momentum vectors are pointing. The second case is an internal singularity, so called because it occurs when the total array momentum is not at the momentum limit (it occurs at a radius of  $h_0$  in momentum space). Saturation singularities cannot be avoided and represent the physical limits of the array. Avoiding internal singularities is the primary focus of all steering laws, because these must be avoided to ensure that the array operates at full capacity<sup>10</sup>.

One way to visually represent the CMG triplet configuration at any moment is through diagrams such as Fig. 2, where gimbal angles are shown. In this case, internal singularities occur when two of the CMGs point in the same direction and the third is directly opposite. An equally valid way to represent the CMG configuration is by the vector sum of the three component vectors, that is, by arranging the three vectors head to tail. Singularities can be seen as cases where the area enclosed by the

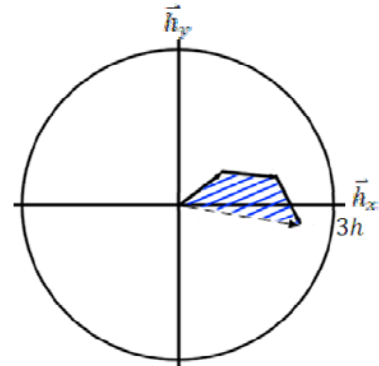


**Figure 3. CMG array in momentum space.** The solid vectors are the momentum vectors of the three CMGs. The dashed vector is the total momentum vector (the vector sum of the three CMG vectors). Blue hatching represents the area enclosed by the three CMG vectors and the total momentum vector.

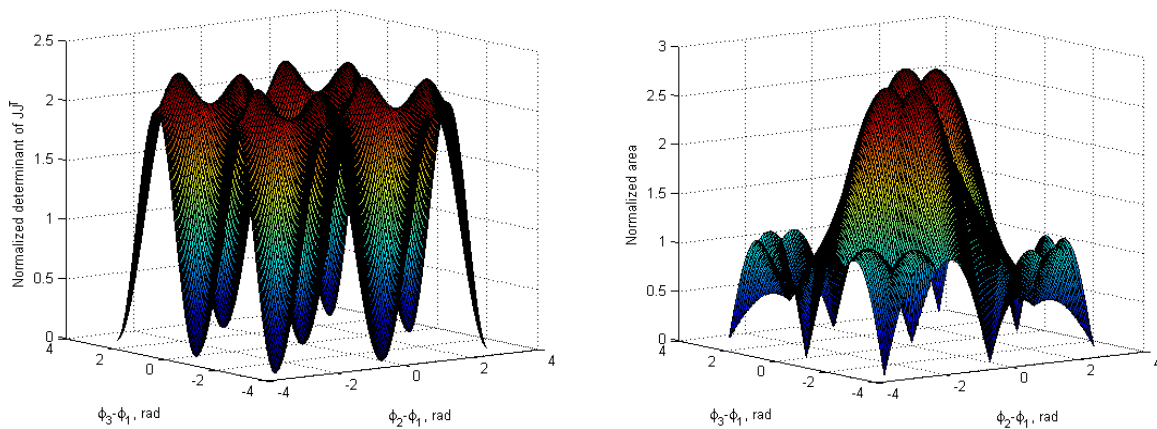


**Figure 4. Determinant of  $JJ^T$  and area between CMG vectors.** Singularities occur when the determinant of  $JJ^T$  is zero. These points coincide with the points at which the area enclosed by the three CMG vectors and the total momentum vector is also zero.

three CMG momentum vectors and the total momentum vector is zero. Note that since the ordering of the CMG vectors is arbitrary, it must be true that all orderings of momentum vectors have zero area for the array to be singular. Figure 3 shows the vector-addition representation.

Figure 4 shows a comparison of the determinant of  $JJ^T$  and the area enclosed by the momentum vectors as defined above. Since the area depends on how the CMGs are ordered, the area shown is always that of the ordering which produces the largest area. The area enclosed by the CMG momentum vectors and the total momentum vector is zero only when the determinant of  $JJ^T$  is zero.

## B. Steering Law

Given the goals of an ideal steering law described in the introduction, a steering law for a triplet CMG array must produce the requested torque while avoiding the gimbal-angle space around the internal singularity. In order to keep the torque produced equal at all times to the torque requested, the gimbal effort used for conditioning the array must be in the null space of  $J$ . The general form for a constrained steering law, further explained in Ref. 8, can be expressed as:

$$\begin{bmatrix} \tau \\ D \end{bmatrix} = \begin{bmatrix} J(\Phi) \\ C \end{bmatrix} \dot{\Phi} \quad (3)$$

where  $C$  is a constraint on the null motion. For the constraint to always avoid singularities, the vector representation of the constraint must always have a component orthogonal to the rows of  $J$ . For example,

$$\begin{aligned} C &= [-\sin(\varphi_1) \quad -\sin(\varphi_2) \quad -\sin(\varphi_3)] \times [\cos(\varphi_1) \quad \cos(\varphi_2) \quad \cos(\varphi_3)] \\ C &= [\sin(\varphi_3 - \varphi_2) \quad \sin(\varphi_1 - \varphi_3) \quad \sin(\varphi_2 - \varphi_1)] \end{aligned} \quad (4)$$

The  $D$  term determines the null motion needed to condition the array. The new matrix formed by the original  $J$  and the appended vector  $C$  is now a square matrix, which allows for its direct inversion to solve for the gimbal rates as long as the matrix is non-singular. Because  $C$  is orthogonal to the two rows of  $J$ , the singularities of the new matrix are simply the singularities of  $J$ .

The steering law presented in this paper aims to use the null space of  $J$  in order to keep the CMG momentum vectors well conditioned to avoid the internal singularity of the triplet configuration. In this particular case, the array is well conditioned if the momentum vectors maintain a trapezoidal configuration (see Fig. 3), while keeping the commanded gimbal rates within the CMG's limits. By keeping this trapezoidal configuration, the area between the CMG momentum vectors and the total momentum vector is never zero (a state which represents the internal singularity). In order to achieve this configuration, the array keeps one of the three CMG vectors parallel to the total momentum vector while the other two CMG vectors form the sides of the trapezoid. All three vectors are only parallel at the saturation singularity, and at the internal singularity at  $1h_0$  the two vectors forming the sides are orthogonal to the vector parallel to the total momentum vector.

When a triplet array crosses through the zero momentum state, the trapezoidal configuration can cause an ambiguity that requires the array to “flip” instantaneously to another position. The constraint is therefore modified such that within a small radius of the zero momentum state, a pseudoinverse rule is used instead. Since the radius in which the pseudoinverse rule is used is much smaller than  $1h_0$ , no problems with singularities are encountered by using the pseudoinverse and the issue of very large gimbal rates near zero momentum is avoided. In our implementation, the pseudoinverse rule is used only within  $0.1h_0$ , which allows for enough null motion between  $0.1h_0$  and  $1h_0$  to properly condition the array. In the general case, the radius should be as small as possible but still large enough so that it is possible to traverse through the zero momentum state without gimbal rates exceeding the limit. The choice of this radius depends on the application-specific requirement on simultaneously available torque and momentum.

Given any total momentum vector within the array's momentum envelope, there are six possible ways to arrange the CMGs such that they are in a trapezoidal configuration and their momentum vectors sum to the same total momentum vector. If the current configuration is not a trapezoid, it is necessary to exert null-space gimbal effort to bring the configuration closer to a trapezoid. The first step is to determine which of the six trapezoid configurations is closest to the current (non-trapezoidal) configuration. That is, determine which trapezoid configuration would

require the least amount of gimbal motion to reach from the current configuration. The next step is to use the constraint equation, for which D is obtained as shown in equation 5.

$$D = \begin{bmatrix} \sin(\varphi_3 - \varphi_2) & \sin(\varphi_1 - \varphi_3) & \sin(\varphi_2 - \varphi_1) \end{bmatrix} K \begin{pmatrix} \begin{bmatrix} \varphi_{1t} \\ \varphi_{2t} \\ \varphi_{3t} \end{bmatrix} - \begin{bmatrix} \varphi_1 \\ \varphi_2 \\ \varphi_3 \end{bmatrix} \end{pmatrix} \quad (5)$$

where  $\varphi_{nt}$  is the gimbal angle the  $n^{\text{th}}$  CMG would have if the array were in the trapezoid configuration closest to the current configuration and K is a 3 by 3 diagonal matrix of gains. The values of the entries of K determine how much effort is used to drive the CMGs to their closest trapezoid configuration.

The gains are chosen such that as much null-space effort as possible is used to keep the array close to a trapezoid without exceeding CMG gimbal limits. The selection of entries in K can be done with numerical iteration: many positive values are evaluated until satisfactory ones are found. Starting with a large value for each non-zero entry in K, the resulting gimbal rates are computed. If the starting values produce gimbal rates that exceed the rate limit, lower values are selected. The values that produce the largest gimbal rates without exceeding the limits are then used to compute D as shown in Eq. 5. This method can be improved upon by stopping the iteration if all the gimbal rates are above a set threshold, or by using a less thorough search if the array is very close to a trapezoid configuration.

The maximum torque the array can produce is a function of how quickly the array can be conditioned when a “worst-case” torque command is applied. While the array does not need to be fully conditioned into a perfect trapezoid configuration, the array must be far enough from a singular configuration when the total momentum is  $1h_0$ . If the array is too far from a trapezoidal configuration when the total momentum crosses  $1h_0$ , gimbal rate limits will be exceeded. For this “worst-case” torque, the magnitude of the torque command must be small enough so that, even after using some of the gimbal motion to meet the requested torque, there is enough gimbal motion left for conditioning the array through null motion. Starting from a zero momentum state, the worst-case torque command is one where minimal time is allowed for conditioning before reaching  $1h_0$  while at the same time causing the gimbal rates required for meeting the torque command to be opposite to the null motion needed for conditioning the array into a trapezoid. As long as the magnitude of the torque command is below the magnitude of the “worst-case” command, the steering law cannot cause the gimbal rates to exceed the limits, and the torque produced will be exactly equal to the torque requested. In most cases, the array will be able to produce more torque than in the worst-case, but since the future torque commands are not known, it is prudent to limit the torque output to what would be available in the worst-case torque command.

### C. Orthogonal Triplet Arrays

Each array of three CMGs using the steering law above is able to produce torque in two directions. In order to produce torque in three dimensions, two triplets are used arranged such that their gimbal directions are orthogonal. The six-CMG array now provides a total momentum envelope that is roughly a  $3h_0$  by  $3h_0$  by  $6h_0$  ellipsoid, as shown in Fig. 5. The extent of the momentum envelope is  $6h_0$  in the direction that is shared between the two triplet arrays. Although this momentum envelope is reachable, zero torque is available at that boundary in the outward direction. Therefore, in practice the momentum is limited to an inner surface at which the required torque is attainable in all directions.

The two arrays can be combined to form a single steering law with two constraints. If, for example, the direction shared between the two arrays is the  $x$ -direction, then the torque equation for the first array is

$$\begin{bmatrix} \tau_x \\ \tau_y \\ D_1 \end{bmatrix} = \begin{bmatrix} J_1 \\ C_1 \end{bmatrix} \begin{bmatrix} \dot{\varphi}_1 \\ \dot{\varphi}_2 \\ \dot{\varphi}_3 \end{bmatrix} \quad (6)$$

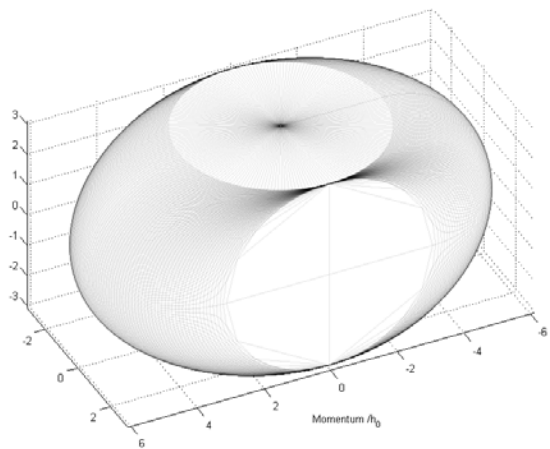


**Figure 5. Momentum envelope for two orthogonal triplets.** The maximum extent is  $6h_0$  in the direction orthogonal to both gimbal axes and  $3h_0$  in the other two directions.

and the torque equation for the second array is

$$\begin{bmatrix} \tau_x \\ \tau_z \\ D_2 \end{bmatrix} = \begin{bmatrix} J_2 \\ C_2 \end{bmatrix} \begin{bmatrix} \dot{\phi}_4 \\ \dot{\phi}_5 \\ \dot{\phi}_6 \end{bmatrix}. \quad (7)$$

The total torque on the spacecraft from the two arrays can be expressed as a sum of the torque from each array, as shown in Eq. 8. Note that the gimbal motion used for conditioning the array (the  $D$  terms) do not carry through to the torque on the spacecraft.

$$\begin{bmatrix} \tau_x \\ \tau_y \\ \tau_z \end{bmatrix} = \begin{bmatrix} 1 & 0 & 0 \\ 0 & 1 & 0 \\ 0 & 0 & 0 \end{bmatrix} \begin{bmatrix} \tau_x \\ \tau_y \\ D_1 \end{bmatrix} + \begin{bmatrix} 1 & 0 & 0 \\ 0 & 0 & 0 \\ 0 & 1 & 0 \end{bmatrix} \begin{bmatrix} \tau_x \\ \tau_z \\ D_2 \end{bmatrix} \quad (8)$$

Rearranging the terms and substituting Eq. 6 and 7, the torque in three dimensions can be expressed as a function of the gimbal rates.

$$\begin{bmatrix} \tau_x \\ \tau_y \\ \tau_z \end{bmatrix} = \begin{bmatrix} 1 & 0 & 0 & 1 & 0 & 0 \\ 0 & 1 & 0 & 0 & 0 & 0 \\ 0 & 0 & 0 & 0 & 1 & 0 \end{bmatrix} \begin{bmatrix} \tau_x \\ \tau_y \\ D_1 \\ \tau_x \\ \tau_z \\ D_2 \end{bmatrix} \quad (9)$$

$$\begin{bmatrix} \tau_x \\ \tau_y \\ \tau_z \end{bmatrix} = \begin{bmatrix} 1 & 0 & 0 & 1 & 0 & 0 \\ 0 & 1 & 0 & 0 & 0 & 0 \\ 0 & 0 & 0 & 0 & 1 & 0 \end{bmatrix} \begin{bmatrix} J_1 & 0 \\ C_1 & 0 \\ 0 & J_2 \\ 0 & C_2 \end{bmatrix} \begin{bmatrix} \dot{\phi}_1 \\ \dot{\phi}_2 \\ \dot{\phi}_3 \\ \dot{\phi}_4 \\ \dot{\phi}_5 \\ \dot{\phi}_6 \end{bmatrix}$$

It is necessary to reintroduce the  $D$  terms to the left hand side of the equation in order to properly solve for the gimbal rates. This is done as shown in Eq. 10.

$$\begin{bmatrix} \tau_x \\ \tau_y \\ \tau_z \\ D_1 \\ D_2 \end{bmatrix} = \begin{bmatrix} 1 & 0 & 0 & 1 & 0 & 0 \\ 0 & 1 & 0 & 0 & 0 & 0 \\ 0 & 0 & 0 & 0 & 1 & 0 \\ 0 & 0 & 1 & 0 & 0 & 0 \\ 0 & 0 & 0 & 0 & 0 & 1 \end{bmatrix} \begin{bmatrix} J_1 & 0 \\ C_1 & 0 \\ 0 & J_2 \\ 0 & C_2 \end{bmatrix} \begin{bmatrix} \dot{\phi}_1 \\ \dot{\phi}_2 \\ \dot{\phi}_3 \\ \dot{\phi}_4 \\ \dot{\phi}_5 \\ \dot{\phi}_6 \end{bmatrix} \quad (10)$$

Equation 10 can now be used to solve for the gimbal rates for the six CMGs using a pseudoinverse.

### III. Steering Law Simulations

#### A. 2-D Single Triplet Simulation

A steering law such as the one presented above must work for arbitrary torque commands less than or equal in magnitude to the required maximum torque capability of the array. The analysis presented here assesses the triplet steering law presented above for one triplet responding to a 2-D torque command. While the steering law can be

tested for any torque command, it is a torque command that minimizes the null space of the array which dictates the maximum torque capability. This worst-case torque command is designed such that the CMG angles are always as far away as possible from the desired trapezoid angles while pushing the array towards the  $1h_0$  state as directly as possible. In this case, the command keeps the trapezoid angles rotating away from the current gimbal angles, effectively causing the current angles to “chase” the trapezoid. The command then switches to one that heads directly outwards, which causes the array to be as nearly singular as possible. Figure 6 shows the gimbal rates commanded by the steering law when given this torque command.

The torque command is shown in the top subplot as its components in the  $x$  and  $y$  directions. The total momentum is shown in the middle subplot, both as total magnitude and components in the  $x$  and  $y$  directions. The CMG gimbal rates are shown in the bottom subplot, where the dashed line represents the gimbal rate limit. Near the time at which the command switches (1.5 seconds) the gimbal rates are very close to their limits. However, the array is able to exert enough null motion to attain a non-singular configuration by the time the total momentum reaches  $1h_0$  (4.1 seconds). Gimbal rate limits are never exceeded, which indicates the array never becomes singular during the simulation.

### B. Violet Nanosatellite and 3-D Simulation Using Orthogonal Triplets

Violet is Cornell University’s entry into the University Nanosat-6 competition. Its primary mission is to test CMG steering laws in orbit. Violet carries eight CMGs of which six can be used simultaneously, allowing for multiple possible array geometries<sup>9</sup>. One of the possible geometries is the six-CMG array described in this paper.

As part of the work for the development of Violet, an attitude control simulation was produced by the team and made available to guest investigators<sup>9</sup>. The steering law presented above will be tested in three-dimensional cases by

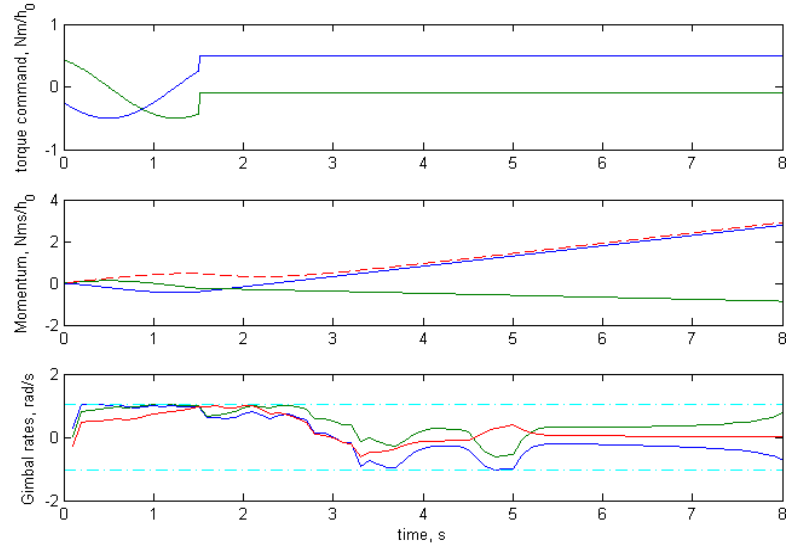


**Figure 6. Triplet steering law simulation.** The top subplot shows the torque commanded as components in two directions. The middle subplot shows the total momentum vector as components in the  $x$  and  $y$  directions. In both the top and middle subplots blue denotes the  $x$ -direction and green the  $y$ -direction. The dashed red in the middle subplot is the magnitude of the total momentum vector. The bottom subplot shows the gimbal rates, with blue being the gimbal rate of the first CMG, green that of the second and red that of the third. The dashed cyan lines are the gimbal rate limits used in this simulation.

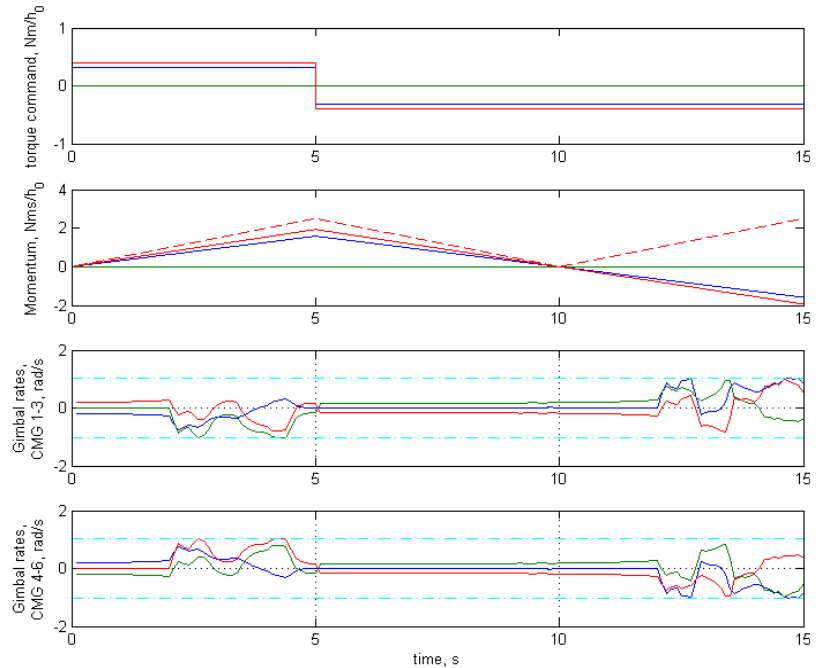


**Figure 7. Orthogonal triplet steering law simulation.** The top subplot shows the torque commanded and the second subplot shows the total momentum vector, both in body coordinates. In both the first and second subplots blue denotes the  $x$ -direction, green the  $y$ -direction and red the  $z$ -direction. The dashed red line in the second subplot is the magnitude of the momentum vector. The bottom two subplots show the gimbal rates for the first and second array. The dashed cyan lines are the rate limits.

commanding test slews using Violet's simulation. These tests would be done in preparation for using the steering law in orbit, were Violet to be launched.

The performance of the steering law for two orthogonal triplets under an example torque command is shown in Figure 7. Torque is commanded in a constant direction for five seconds, after which the command is reversed. This command demonstrates the six-CMG array crossing through the  $1h_0$  radius and then back through the zero momentum state. The three components of the commanded torque are shown in the top subplot, the three components of momentum as well as the magnitude of the total momentum vector are shown in the second subplot and the gimbal rates are shown in the third and fourth subplot. A coordinate system matching that of the Violet satellite is used for the torque and momentum vectors. In the Violet body frame, the first array (CMG 1 – 3) has a gimbal axis direction of  $\begin{bmatrix} 0 & \sqrt{2}/2 & \sqrt{2}/2 \end{bmatrix}^T$  and the second array (CMG 4 – 6) has a gimbal axis of  $\begin{bmatrix} 0 & -\sqrt{2}/2 & \sqrt{2}/2 \end{bmatrix}^T$ . In the simulation shown in Fig. 7, the gimbal rate limit is not exceeded in either array, and the transition through the zero momentum state (which occurs at 10s) does not cause large gimbal rates.

#### IV. Conclusions

The key concept of analyzing singularities from a geometrical standpoint greatly simplifies the process of determining suitable singularity-free steering laws. While many previous publications are concerned with avoiding singular configurations because of the introduction of torque errors, a better metric would assess whether the gimbal rates are less than the maximum rate at which the CMG can rotate. The use of the null space to condition the array while keeping the total momentum vector unchanged allows for an instantaneous steering law that does not exceed gimbal rate limits and does not introduce torque errors as long as the commanded torque is below a maximum value. Simulations show that the maximum torque value can be determined by commanding a torque which leaves as little gimbal motion as possible for null-space maneuvering. Extensions of this work will include a more rigorous validation using Monte Carlo simulations of arbitrary torque commands while keeping the total array momentum within the momentum envelope.

#### References

- <sup>1</sup> Peck, M.A. "Low-Power, High-Agility Space Robotics" *AIAA Guidance, Navigation and Control Conference and Exhibit*, San Francisco, CA, Aug 15-18, 2005.
- <sup>2</sup> Wie, B., "Singularity Analysis and Visualization for Single-Gimbal Control Moment Gyro Systems," *Journal of Guidance, Control, and Dynamics*, Vol. 27, No. 2, 2004, pp. 271–282.
- <sup>3</sup> Peck, Paluszek, Thomas, and Mueller, "Control-Moment Gyroscopes for Joint Actuation: A New Paradigm in Space Robotics," *AIAA 1st Space Exploration Conference*, Orlando, FL, Jan 30 - Feb 1, 2005
- <sup>4</sup> Carpenter, M.A. and Peck, M.A. "Dynamics of a High-Agility, Low-Power Imaging Payload" *IEEE Transactions on Robotics*, Vol. 24, No. 3, 2008, pp. 666-675.
- <sup>5</sup> Lappas, V. J., Steyn, W. H., and Underwood, C. I., "Attitude Control for Small Satellites Using Control Moment Gyros," *Acta Astronautica*, Vol. 51, Nos. 1–9, 2002, pp. 101–111.
- <sup>6</sup> McMickell, B. M., Davis, P., Schudrowitz, C., Leve, F. "A Momentum Control System for Agile Responsive Space Satellites" *AIAA 8<sup>th</sup> Responsive Space Conference*, Los Angeles, CA, March 8-11, 2010.
- <sup>7</sup> Kurokawa, H. "Survey of Theory and Steering Laws of Single-Gimbal Control Moment Gyros" *Journal of Guidance, Control, and Dynamics*, Vol. 30, No. 5, Sept.-Oct. 2007, pp. 1331-1340.
- <sup>8</sup> Jones, L.L. and Peck, M.A. "A Generalized Framework for Linearly-Constrained Singularity-Free Control Moment Gyro Steering Laws" *AIAA Guidance, Navigation and Control Conference*, Chicago, IL, Aug 10-13, 2009.
- <sup>9</sup> Gersh, J. and Peck, M.A. "Violet: A High-Agility Nanosatellite for Demonstrating Small Control-Moment Gyroscopes Prototypes and Steering Laws" *AIAA Guidance, Navigation and Control Conference*, Chicago, IL, Aug 10-13, 2009.
- <sup>10</sup> Hamilton, B. Underhill, B. "Modern Momentum Systems for Spacecraft Attitude Control" *29<sup>th</sup> AAS Guidance and Control Conference*, Breckenridge, CO, Feb 4-8, 2006.